NACA

CASE FILE COPY

RESEARCH MEMORANDUM

PRESSURE-DISTRIBUTION MEASUREMENTS OVER AN EXTENSIBLE

LEADING-EDGE FLAP ON TWO WINGS HAVING LEADING-

EDGE SWEEP OF 42° AND 52°

By

Reino J. Salmi

Langley Aeronautical Laboratory
Langley Air Force Base, Va.

NATIONAL ADVISORY COMMITTEE
FOR AERONAUTICS

WASHINGTON

March 7, 1949

RESTRICTED

NATIONAL ADVISORY COMMITTEE FOR AERONAUTICS

RESEARCH MEMORANDUM

PRESSURE—DISTRIBUTION MEASUREMENTS OVER AN EXTENSIBLE

LEADING—EDGE FLAP ON TWO WINGS HAVING LEADING—
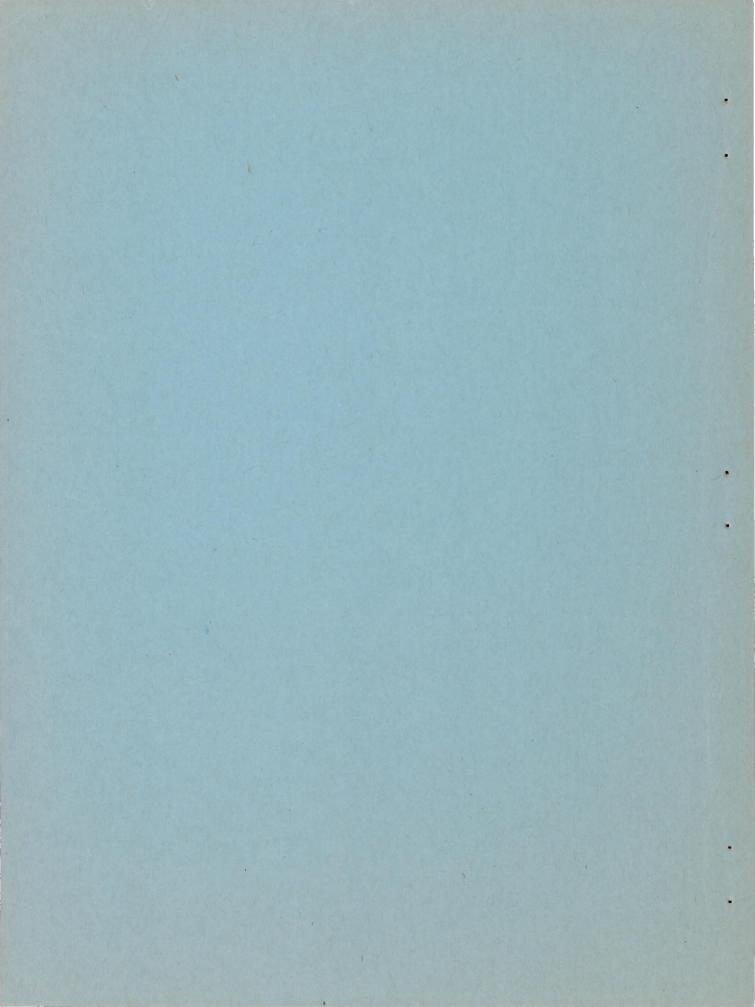
EDGE SWEEP OF 42° AND 52°

By Reino J. Salmi

SUMMARY

An investigation of the pressure distribution over a leading—edge flap was conducted in the Langley 19—foot pressure tunnel. The tests were made on 42° and 52° sweptback wings of NACA 64_1—112 sections, the 42° wing being used in conjunction with a circular cross—section fuselage in a high—wing combination. The pressure—distribution data for the 52° swept—back wing were obtained at various angles of attack and angles of yaw for a Reynolds number of 4.4×10^6 and a Mach number of 0.08, for both split flaps deflected and neutral configurations with upper—surface fences installed. The 42° sweptback wing was tested at zero yaw for various angles of attack at a Reynolds number of 5.12×10^6 and a Mach number of 0.11 with split flaps deflected.

The pressure—distribution measurements over the leading—edge flap indicated that the rate of increase of the flap normal—force coefficient C_{N_f} with lift coefficient was nearly constant for the conditions tested, but the hinge—moment coefficient C_{h_f} increased with lift coefficient at an increasing rate. The maximum values of C_{N_f} and C_{h_f} obtained at zero yaw with the split flaps deflected were 3.24 and 1.62, respectively, for the 42° sweptback wing, and 3.12 and 1.68, respectively, for the 52° sweptback wing. The maximum values of C_{N_f} and C_{h_f} were lower when the split flaps were neutral. Yawing the 52° sweptback wing increased the maximum values of C_{N_f} and C_{h_f} on the leading wing panel and caused a decrease for the trailing wing panel.

INTRODUCTION

Experimental investigations such as references 1 and 2 have shown that extensible leading—edge flaps can increase the maximum lift and improve the stability characteristics of sweptback wings. Practical application of such flaps on any aircraft would require some knowledge

of the magnitudes of the aerodynamic forces on the flaps. Pressure—
distribution measurements were therefore made over a leading—edge flap
on two wings of 42° and 52° sweepback. The 42° sweptback wing had
NACA 64_1—112 airfoil sections normal to the 0.273 chord line and the
52° sweptback wing had the same sections normal to the 0.282 chord line.
(The 0.273 and 0.282 chord lines correspond to the 0.25 chord line of a
similar wing panel which has zero sweep at the 0.25 chord line.) Both
wings had taper ratios of 0.625 but differed in aspect ratio, the 42° wing
having an aspect ratio of 4.01 and the 52° wing an aspect ratio
of 2.88. In addition to showing the effect of yaw on the leading—edge
flap loads, the results at various yaw angles might be used in the
prediction of leading—edge flap loads on wings of different sweepback.
The original data obtained on the 42° swept wing, previously published
in reference 3, have also been included in this report for purposes of
comparison.

COEFFICIENTS AND SYMBOLS

α angle of attack of wing chord line measured in a plane
parallel to the plane of symmetry

Λ sweep angle of wing leading edge

ψ angle of yaw, positive when right wing is back

C_L lift coefficient (Lift/qS)

C_D drag coefficient (Drag/qS)

C_m pitching—moment coefficient referred to quarter—chord
point of mean aerodynamic chord (Moment/$qS\overline{c}$)

c_{n_f} section normal—force coefficient of leading—edge
flap $\left(\int P\, d\left(\dfrac{x}{c_f}\right) \right)$

C_{N_f} normal—force coefficient of complete leading—edge
flap $\left(\int c_{n_f}\, d\left(\dfrac{y_f}{b_f}\right) \right)$

c_{h_f} section hinge—moment coefficient of leading—edge flap
about trailing edge of flap $\left(\int P\, \dfrac{x}{c_f}\, d\left(\dfrac{x}{c_f}\right) \right)$

C_{h_f} hinge—moment coefficient of complete leading—edge flap
about trailing edge of flap $\left(\int c_{h_f}\, d\left(\dfrac{y_f}{b_f}\right) \right)$

c.p.   center of pressure of leading—edge flap in percent of
                    flap chord measured from leading edge of

$$\text{flap} \left(100 \left(1 - \frac{c_{h_f}}{c_{n_f}} \right) \right)$$

R   Reynolds number (based on wing mean aerodynamic chord)

S   wing area

q   free—stream dynamic pressure

$\bar{c}$ wing mean aerodynamic chord

c'   wing chord normal to 0.273 chord line of 42° wing and
                    0.282 chord line of 52° wing

p   local static pressure

P   pressure coefficient $\left(\dfrac{p - p_o}{q} \right)$

p_o free—stream static pressure

y_f distance measured along span of leading—edge flap from
                    inboard end

b_f span of leading—edge flap

x   distance measured along leading—edge—flap chord from
                    trailing edge of flap (perpendicular to leading edge
                    of flap)

c_f leading—edge—flap chord measured perpendicular to flap
                    leading edge.

MODELS

The models used in the present tests had been previously used in
the investigations reported in references 1 and 2, in which they are
described in detail. Figure 1 shows the location of the leading—edge
flaps on each of the models and also the geometric parameters of the
models. The 42° sweptback wing had NACA 64_1–112 airfoil sections normal
to the 0.273 chord line, and the 52° wing had the same sections normal
to the 0.282 chord line. (The 0.273 and 0.282 chord lines correspond
to the 0.25 chord line of a similar wing panel which has zero sweep at

the 0.25 chord line .) The 42° wing had an aspect ratio of 4.01 and the
52° wing, 2.88. Both wings had taper ratios of 0.625. The 42° wing was
tested with half–span split flaps and in combination with a circular
cross–section fuselage of fineness ratio 10 to 1. The 52° sweptback wing
was also tested with half–span split flaps and an upper–surface fence,
which made the wing longitudinally stable. The fence was located 45 per–
cent of the semispan from the plane of symmetry, had a constant height
of 6 percent of the local airfoil chord, and extended over the rear 95 per–
cent of the chord. The same leading–edge flaps were used on both
models with equal deflection angles of 50° from the wing chord plane being
maintained. The geometry of the flaps and the location of the orifices,
which were on the right–hand flap only, are given in figure 2. Figure 3
shows photographs of the 42° and 52° sweptback wings in the Langley 19–foot
pressure tunnel.

TESTS

The tests were made in the Langley 19–foot pressure tunnel with the
air compressed to approximately 33 pounds per square inch absolute. The
flap pressures were recorded photographically from a multiple–tube manometer.
The 52° sweptback wing was mounted on the single–support system, and
the data were obtained at yaw angles of 10°, 0°, –10°, and –20° at
various angles of attack for the split flaps both deflected and neutral.
The 42° sweptback wing was mounted on a two–support system and was tested
in conjunction with a fuselage, forming a high–wing combination. The
flap pressure data were obtained at zero yaw for various angles of attack
for the split–flaps–deflected configuration only.

The pressure data for the 52° wing were obtained at a Reynolds number
of 4.4×10^6 with a corresponding Mach number of 0.08, and the tests on
the 42° wing were made at a Reynolds number of 5.12×10^6 with a corre–
sponding Mach number of 0.14.

The force data presented were obtained with all connector tubing
removed. The usual wind–tunnel corrections (the same as in references 1
and 2) were applied.

RESULTS AND DISCUSSION

The lift, drag, and pitching–moment characteristics of both the
42° and 52° sweptback wings are presented in figure 4. The chordwise
pressure distributions for each of the five spanwise stations along the
leading–edge flap are given in figure 5 for the 42° sweptback wing and
in figures 6 and 7 for the 52° sweptback wing. The dotted portions of
some of the curves of figure 5 are interpolations based on the existing
data, as no data were obtained for the lower surface of the flap at those

sections. Pressure coefficients obtained along the lower surface were
faired point to point and no attempt to reach stagnation pressure was
made since the effect on the force coefficient would be negligible.

Figures 5 to 7 show that at the lowest angles of attack the flap
loads for both the 42° and 52° sweptback wings were small and were concen-
trated near the trailing edge of the flap. As the angle of attack was
increased, large negative pressure peaks developed at the leading edge
of the flaps, accompanied by a forward movement in the center of pressure.
A maximum value of negative pressure coefficient measured was -10.75 for
the 52° sweptback wing at the 72-percent flap span station (measured
outboard from the inboard end of the flap) at an angle of attack of 25.2°
and zero yaw with the split flaps deflected. It is believed that the
fence would not appreciably affect the pressures on the leading-edge flap.
It is also believed that the pressure distribution over the fuselage on
the 42° sweptback wing has a negligible effect on the pressures over the
leading-edge flap since the model was tested at zero yaw.

The spanwise variations of the flap normal-force and hinge-moment
coefficients for the 42° and 52° sweptback wings are presented in figures 8
to 10. The supporting members of a flap are usually designed for the
maximum load obtainable on the flap, and, therefore, the span-load distri-
bution in the higher angle-of-attack range will be of most interest.
Figures 8 to 10 indicate that the loading was, in general, well distrib-
uted over the flap and that the maximum loading was near the center of
the flap, being shifted slightly toward the inboard end by negative yaw
(which tends to decrease the sweep angle) and toward the outboard side
for positive yaw. The spanwise center of loading was determined for the
configurations at zero yaw and was found to vary from about 45 percent
of the flap span at low angles of attack to about 50 percent in the high
angle-of-attack range.

The normal-force and hinge-moment coefficients of the leading-edge
flap are presented as functions of the lift coefficient in figure 11.
The lift coefficients for the right wing panel of the 52° sweptback wing
were estimated for various angles of yaw from the following empirical
relationship:

$$C_{L_{(yawed\ panel)}} = C_{L_{(\psi=0)}} \left[\frac{\cos(\Lambda + \psi)}{\cos \Lambda} \right]^{0.92}$$

This relationship gave satisfactory agreement when used to check values
of lift coefficient obtained from pressure-distribution measurements of
a 45° sweptback wing at various angles of yaw (reference 4) and was con-
sidered sufficiently accurate (see fig. 12) for presenting the flap load
data.

Figure 11 shows that in general the rate of increase of the normal-
force coefficient with lift coefficient was nearly constant for the
conditions tested.

The figure also shows that the hinge—moment coefficient increased with lift coefficient but at an increasing rate. The hinge—moment curves were nearly parallel, however, for identical trailing—edge—flap configurations. In general, deflecting the split flaps resulted in a marked decrease in the leading—edge flap normal—force and hinge—moment coefficients at constant lift coefficient. Since the split flaps were of partial—span, the lift at the inboard end of the wing would be increased, whereas the outboard half would be carrying a smaller load, thereby reducing the leading—edge flap loads. The inboard end of the leading—edge flap may also be affected by the change in chordwise pressure distribution, due to the split flap.

For any given lift coefficient, the values of the normal—force and hinge—moment coefficients varied considerably with sweepback and yaw. Figure 11 shows that an increase of about 0.30 and 0.32 occurred for C_{N_f} and C_{h_f}, respectively, for an increase in sweepback from 42° to 52°. The coefficients C_{N_f} and C_{h_f} also increased with angle of yaw, for constant lift coefficient, in the range of yaw angles from $\psi = -20^{\circ}$ to $\psi = 10^{\circ}$, so that the incremental increase for each 10° of yaw was greater.

The effects due to yaw or sweepback can be explained quite readily when it is realized that the forces on the flap and the lift of the wing are proportional to the dynamic pressure normal to the leading edge. The rate of increase of the flap normal force with lift coefficient would, therefore, be constant, regardless of the sweep angle if all secondary effects, such as cross flow over the wing, are neglected. However, the curves showing the variation of the flap normal force with lift would be displaced by an amount depending on the sweep angle. The flap was deflected down 50°, and a negative force proportional to the dynamic pressure normal to the leading edge acted upon it when the wing was at zero lift. Since the angle of attack for zero lift is unaffected by sweep, the initial force at zero lift would be changed by varying the sweep angle.

The maximum values of the normal—force and hinge—moment coefficients obtained on the 52° wing varied with angle of yaw and trailing—edge—flap deflection. Figure 13 shows that the maximum values of C_{N_f} and C_{h_f} at zero yaw were about 3.12 and 1.68, respectively, for the split—flaps—deflected configuration and that a decrease of about 0.65 in C_{N_f} and 0.30 in C_{h_f} occurred for 10° of yaw. For the negative yaw angles, an increase of approximately 0.34 in C_{N_f} and 0.05 in C_{h_f} occurred for -20° of yaw. At all angles of yaw, the maximum values of C_{N_f} and C_{h_f} were lower when the split flaps were neutral.

When the 52° sweptback wing was yawed -10°, the angle of sweepback of the right wing panel was equal to the sweepback of the 42° sweptback wing at zero yaw. From figure 11 it can be seen that the curves of C_{N_f} and C_{h_f} against C_L for the two conditions are in fairly good agreement

when the differences in the two model configurations are considered. If the data for the 42° wing had been obtained without a fuselage, it is expected that the agreement would be better, since the lift coefficients would be increased. The maximum values of C_{N_f} and C_{h_f} for the 42° wing were 3.24 and 1.62, which were about equal to the values for the 52° wing at −10° yaw.

The maximum load on a similar flap on any sweptback wing could probably be estimated from the data contained herein. However, particular attention should be given to any devices, such as trailing-edge flaps, which affect the spanwise loading of the wing and also to the original deflection angle of the flap (with respect to the wing chord line), the effect of which was not isolated in this report.
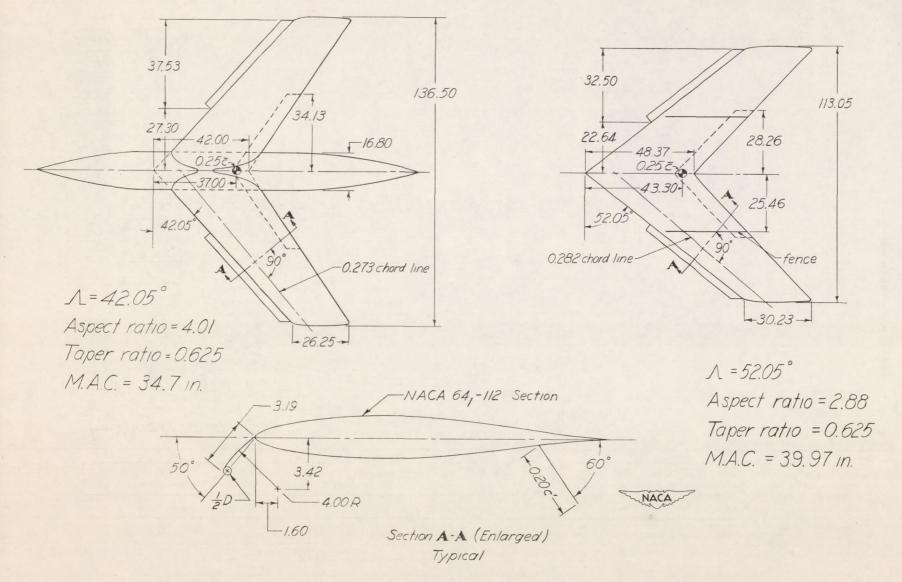
CONCLUSIONS

An investigation of the pressure distribution over an extended leading-edge flap on wings of 42° and 52° sweepback indicated that:

1. The rate of increase of the normal-force coefficient C_{N_f} with lift coefficient was nearly constant for the conditions tested, but the hinge-moment coefficient C_{h_f} increased with lift coefficient at an increasing rate.

2. The maximum values of C_{N_f} and C_{h_f} obtained at zero yaw with the split flaps deflected were 3.24 and 1.62, respectively, for the 42° sweptback wing, and 3.12 and 1.68, respectively, for the 52° sweptback wing.

3. The maximum values of the normal-force and hinge-moment coefficients for the leading-edge flap were lower when the split flaps were neutral.

4. Yawing the 52° sweptback wing increased the maximum values of C_{N_f} and C_{h_f} on the leading wing panel and caused a decrease for the trailing wing panel.
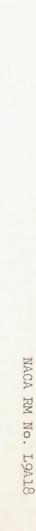
Langley Aeronautical Laboratory
    National Advisory Committee for Aeronautics
        Langley Air Force Base, Va.

REFERENCES

1. Salmi, Reino J.: Yaw Characteristics of a 52° Sweptback Wing of
   NACA 64_1–112 Section with a Fuselage and with Leading–Edge and
   Split Flaps at Reynolds Numbers from 1.93×10^6 to 6.00×10^6.
   NACA RM No. L8H12, 1948.

2. Graham, Robert R., and Conner, D. William: Investigation of High–Lift
   and Stall–Control Devices on an NACA 64–Series 42° Sweptback Wing
   with and without Fuselage. NACA RM No. L7G09, 1947.

3. Conner, D. William, and Foster, Gerald V.: Investigation of Pressure
   Distribution over an Extended Leading–Edge Flap on a 42° Sweptback
   Wing. NACA RM No. L7J03, 1947.

4. Jacobs, W.: Druckverteilungsmessungen an zwei Pfeilflügeln konstanter
   Tiefe ($\varphi = 30°$, $45°$) bei unsymetrischer Anströmung. UM Nr. 2110,
   Deutsche Luftfahrtforschung (Braunschweig), 1944.

37.53

136.50

27.30

34.13

42.00

16.80

0.25č

37.00

42.05°

A

90°

A

0.273 chord line

$\Lambda = 42.05°$

Aspect ratio = 4.01

Taper ratio = 0.625

M.A.C. = 34.7 in.

26.25

32.50

113.05

22.64

48.37

28.26

0.25č

43.30

25.46

52.05°

90°

0.282 chord line

A

A

fence

30.23

$\Lambda = 52.05°$

Aspect ratio = 2.88

Taper ratio = 0.625

M.A.C. = 39.97 in.

NACA 64$_1$-112 Section

3.19

50°

60°

3.42

0.020č

$\frac{1}{2}$ D

4.00 R

1.60

Section **A-A** (Enlarged)

Typical

NACA

Figure 1.— Geometry of 42° and 52° sweptback wing models. All dimensions in inches.

$b_f = 52.70$

49.67

38.15

26.65

15.14

$.363$

$42°$

A

A

Tip

Wing leading edge

Spanwise orifice location

X

Y

0.25

0.10

$c_f = 3.42$

Section A~A   Chordwise orifice location

X	Y
0.24	-0.26
.03	- .13
.03	.13
.27	.38
.60	.52
1.12	.60
1.76	.60
2.52	.47
3.25	.20
.96	.39
2.80	.19

Wing chord line

NACA
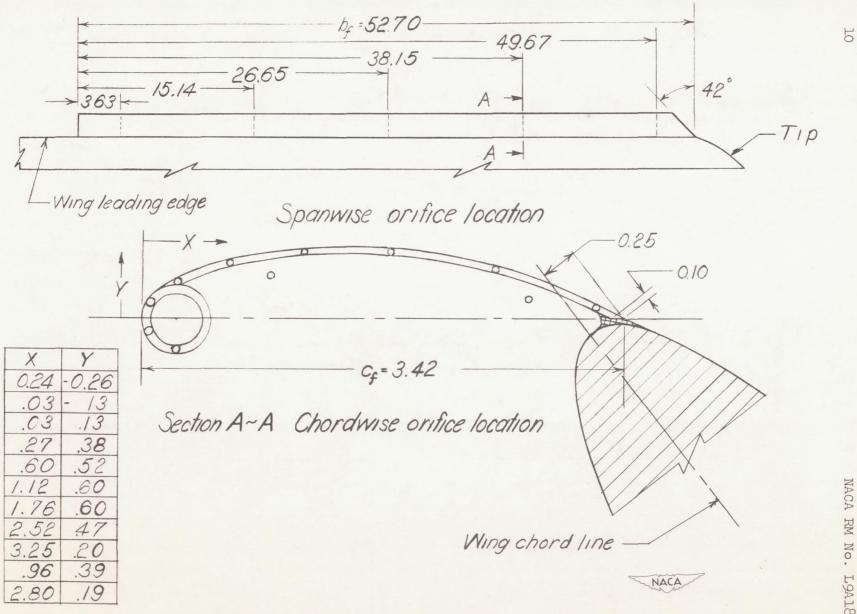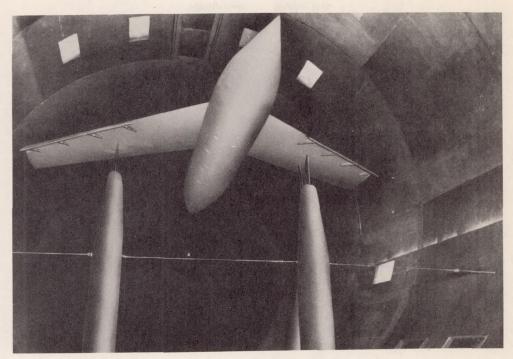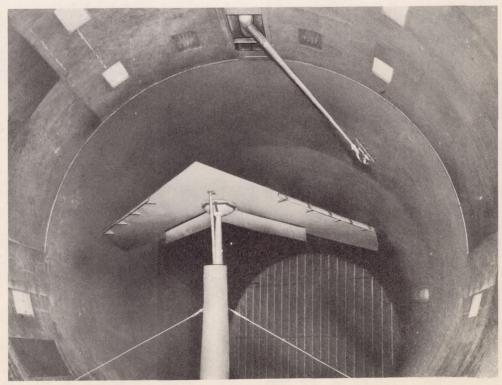
Figure 2.— Location of orifices on leading-edge flap. (All dimensions in inches.)
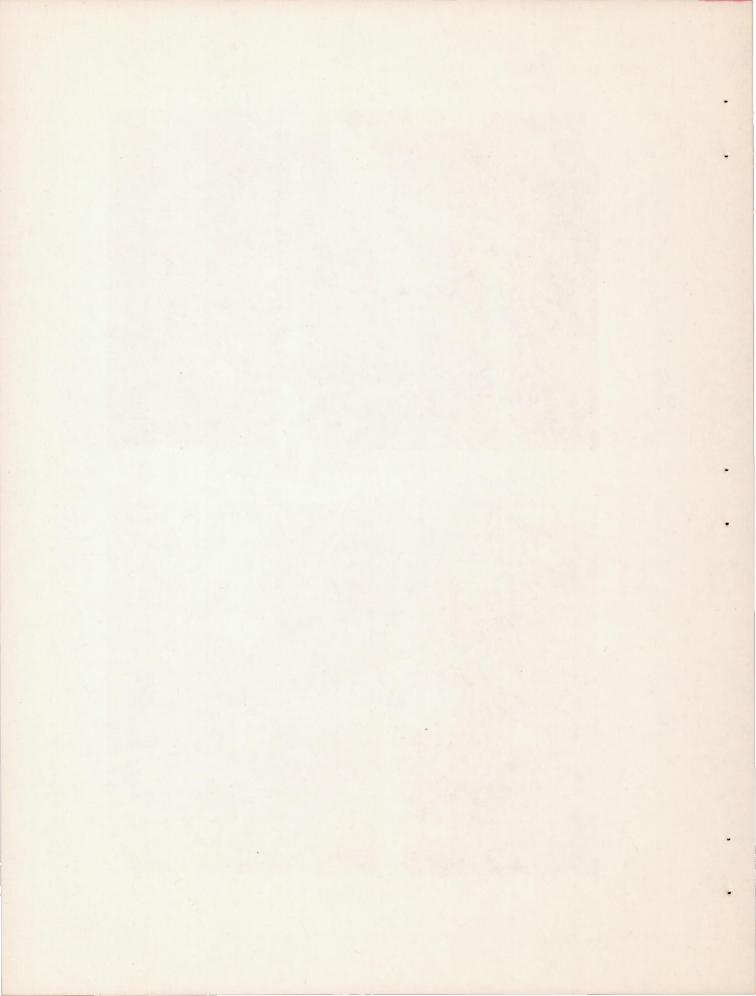
(a) 42° sweptback wing.
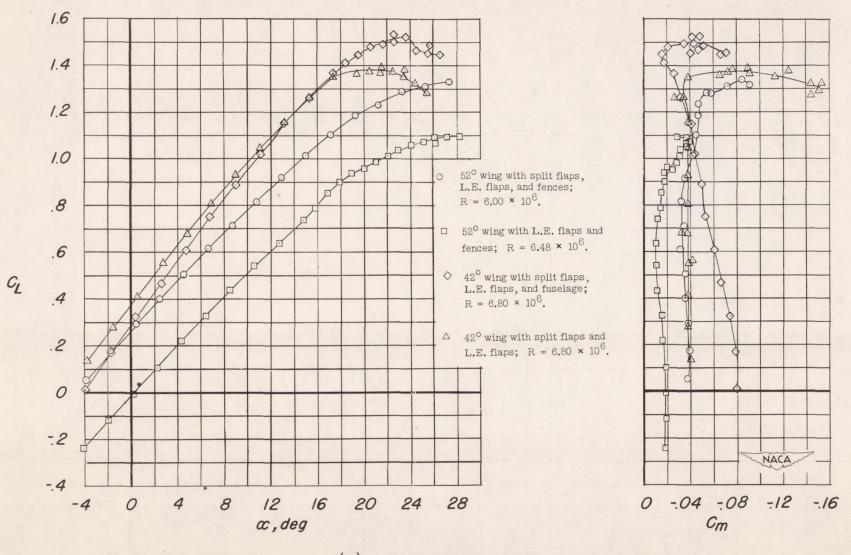
(b) 52° sweptback wing.

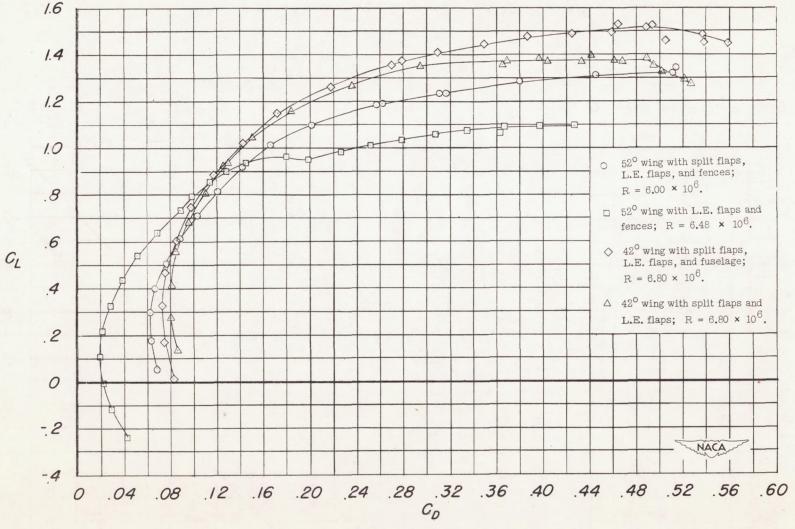Figure 3.— Photographs showing the 42° and 52° sweptback wings.

L-59049

O 52° wing with split flaps,
   L.E. flaps, and fences;
   R = 6.00 × 10⁶.

□ 52° wing with L.E. flaps and
   fences; R = 6.48 × 10⁶.

◇ 42° wing with split flaps,
   L.E. flaps, and fuselage;
   R = 6.80 × 10⁶.

△ 42° wing with split flaps and
   L.E. flaps; R = 6.80 × 10⁶.

(a) C_L against α and C_m.

Figure 4.— Aerodynamic characteristics of the 42° and 52° sweptback
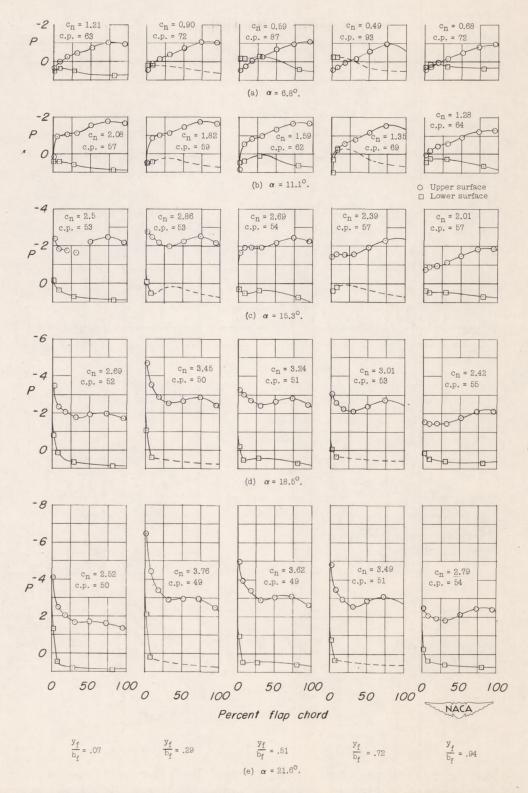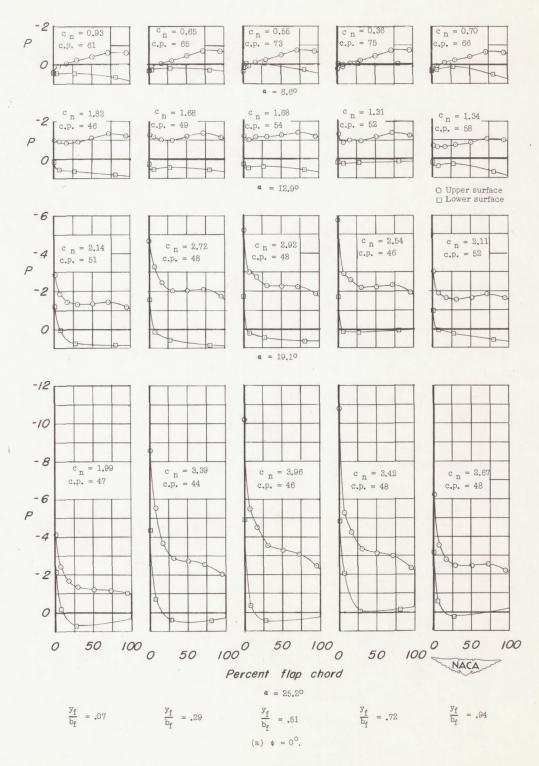wing models.

(b) C_L against C_D.

Figure 4.— Concluded.

Figure 5.— Chordwise pressure distribution over the leading—edge flap on the 42° sweptback wing at five spanwise stations. Split flaps deflected; R = 5.12 × 10⁶.

-2
P

$c_n = 0.93$
$c.p. = 61$

$c_n = 0.65$
$c.p. = 65$

$c_n = 0.55$
$c.p. = 73$

$c_n = 0.38$
$c.p. = 75$

$c_n = 0.70$
$c.p. = 66$

0

$\alpha = 6.6^{o}$

-2
P

$c_n = 1.82$
$c.p. = 46$

$c_n = 1.68$
$c.p. = 49$

$c_n = 1.68$
$c.p. = 54$

$c_n = 1.31$
$c.p. = 52$

$c_n = 1.34$
$c.p. = 58$

0

$\alpha = 12.9^{o}$

O Upper surface
□ Lower surface

-6

-4
P

$c_n = 2.14$
$c.p. = 51$

$c_n = 2.72$
$c.p. = 48$

$c_n = 2.92$
$c.p. = 48$

$c_n = 2.54$
$c.p. = 46$

$c_n = 2.11$
$c.p. = 52$

-2

0

$\alpha = 19.1^{o}$

-12

-10

-8

$c_n = 1.99$
$c.p. = 47$

$c_n = 3.39$
$c.p. = 44$

$c_n = 3.96$
$c.p. = 46$

$c_n = 3.42$
$c.p. = 48$

$c_n = 2.67$
$c.p. = 48$

-6
P

-4

-2

0

$0 \quad 50 \quad 100$ $0 \quad 50 \quad 100$ $0 \quad 50 \quad 100$ $0 \quad 50 \quad 100$ $0 \quad 50 \quad 100$

NACA

Percent flap chord

$\alpha = 25.2^{o}$

$\dfrac{y_f}{b_f} = .07$ $\dfrac{y_f}{b_f} = .29$ $\dfrac{y_f}{b_f} = .51$ $\dfrac{y_f}{b_f} = .72$ $\dfrac{y_f}{b_f} = .94$

(a) $\psi = 0^{o}$.

Figure 6.— Chordwise pressure distribution over the leading—edge flap on the 52° sweptback wing at five spanwise stations. Split flaps deflected and fences installed; $R = 4.4 \times 10^{6}$.
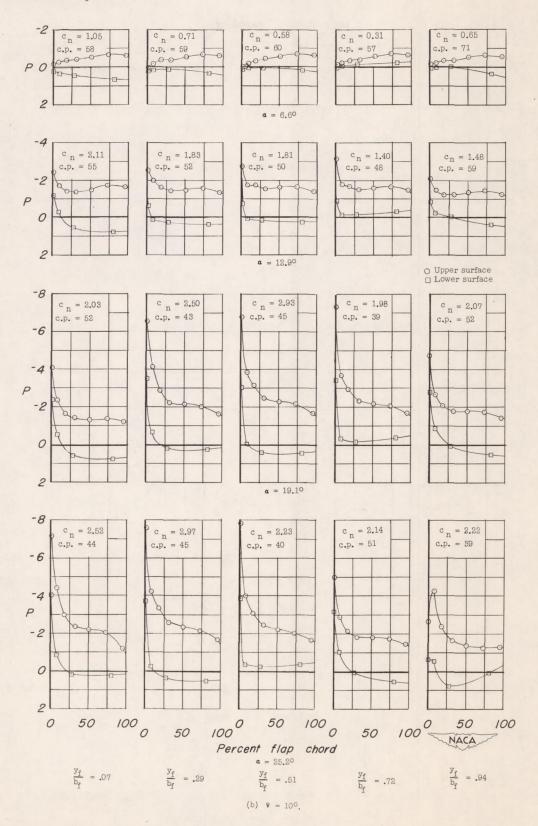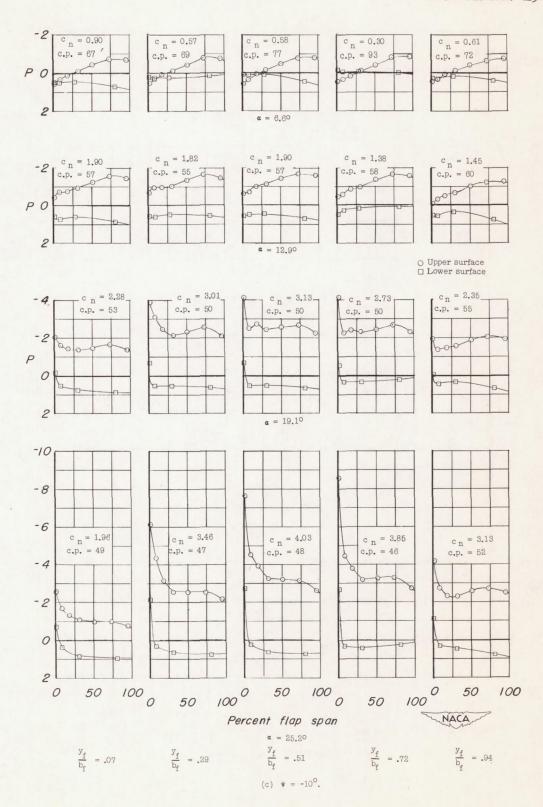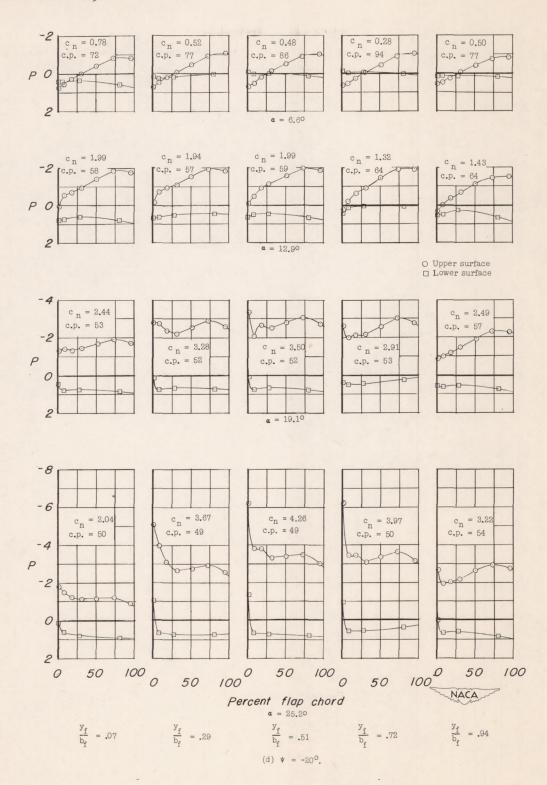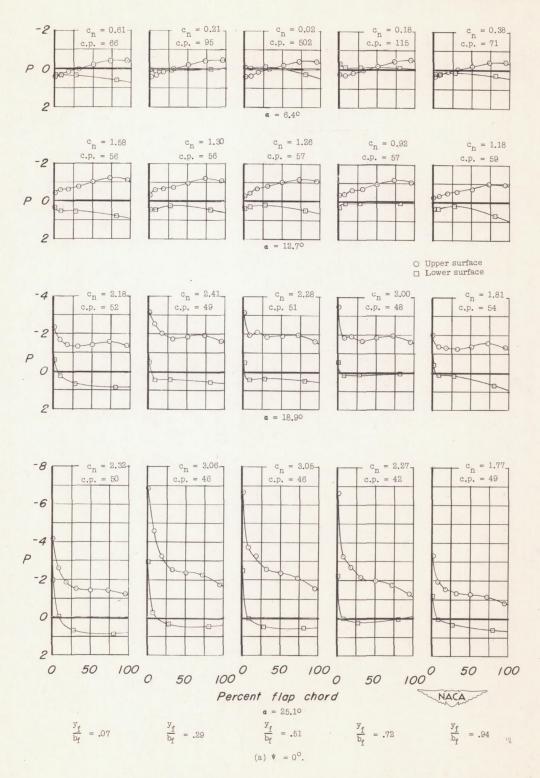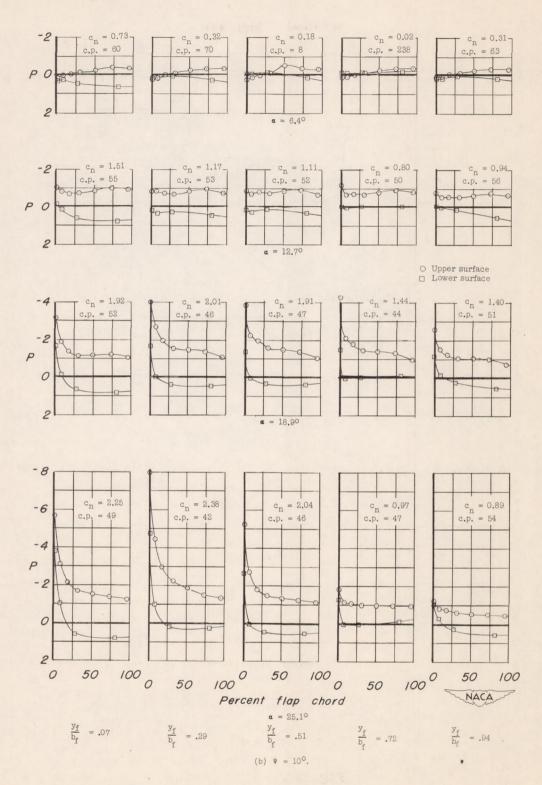
O Upper surface
□ Lower surface

Percent flap chord

α = 25.2°

$\frac{y_f}{b_f} = .07$ $\frac{y_f}{b_f} = .29$ $\frac{y_f}{b_f} = .51$ $\frac{y_f}{b_f} = .72$ $\frac{y_f}{b_f} = .94$

(b) Ψ = 10°.

Figure 6.— Continued.

$c_n = 0.90$
c.p. = 67

$c_n = 0.57$
c.p. = 69

$c_n = 0.58$
c.p. = 77

$c_n = 0.30$
c.p. = 93

$c_n = 0.61$
c.p. = 72

P

$\alpha = 6.6^{\circ}$

$c_n = 1.90$
c.p. = 57

$c_n = 1.82$
c.p. = 55

$c_n = 1.90$
c.p. = 57

$c_n = 1.38$
c.p. = 58

$c_n = 1.45$
c.p. = 60

P

$\alpha = 12.9^{\circ}$

○ Upper surface
□ Lower surface

$c_n = 2.28$
c.p. = 53

$c_n = 3.01$
c.p. = 50

$c_n = 3.13$
c.p. = 50

$c_n = 2.73$
c.p. = 50

$c_n = 2.35$
c.p. = 55

P

$\alpha = 19.1^{\circ}$

$c_n = 1.96$
c.p. = 49

$c_n = 3.46$
c.p. = 47

$c_n = 4.03$
c.p. = 48

$c_n = 3.85$
c.p. = 46

$c_n = 3.13$
c.p. = 52

0   50   100   0   50   100   0   50   100   0   50   100   0   50   100

Percent flap span

$\alpha = 25.2^{\circ}$

$\dfrac{y_f}{b_f} = .07$ $\dfrac{y_f}{b_f} = .29$ $\dfrac{y_f}{b_f} = .51$ $\dfrac{y_f}{b_f} = .72$ $\dfrac{y_f}{b_f} = .94$

(c) $\psi = -10^{\circ}$.

NACA

Figure 6.— Continued.

(d) ψ = -20°.

Figure 6.— Concluded.

Figure 7.— Chordwise pressure distribution over the leading—edge flap on the 52° sweptback wing at five spanwise stations. Split flaps neutral, fences installed; R = 4.4 × 10⁶.
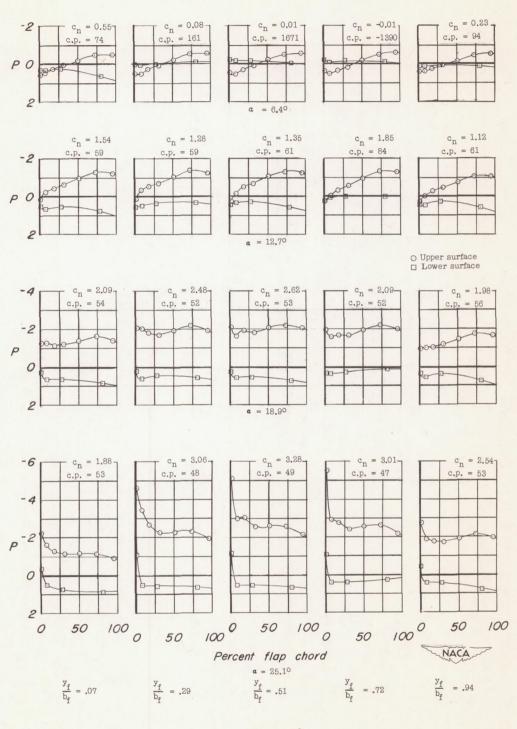
Figure 7.— Continued.

$c_n = 0.55$
c.p. = 74

$c_n = 0.08$
c.p. = 161

$c_n = 0.01$
c.p. = 1671

$c_n = -0.01$
c.p. = -1390

$c_n = 0.23$
c.p. = 94

$\alpha = 6.4^\circ$

$c_n = 1.54$
c.p. = 59

$c_n = 1.28$
c.p. = 59

$c_n = 1.35$
c.p. = 61

$c_n = 1.85$
c.p. = 84

$c_n = 1.12$
c.p. = 61

$\alpha = 12.7^\circ$

○ Upper surface
□ Lower surface

$c_n = 2.09$
c.p. = 54

$c_n = 2.48$
c.p. = 52

$c_n = 2.62$
c.p. = 53

$c_n = 2.09$
c.p. = 52

$c_n = 1.98$
c.p. = 56

$\alpha = 18.9^\circ$

$c_n = 1.88$
c.p. = 53

$c_n = 3.06$
c.p. = 48

$c_n = 3.28$
c.p. = 49

$c_n = 3.01$
c.p. = 47

$c_n = 2.54$
c.p. = 53

0   50   100   0   50   100   0   50   100   0   50   100   0   50   100

Percent flap chord

$\alpha = 25.1^\circ$

$\frac{y_f}{b_f} = .07$ $\frac{y_f}{b_f} = .29$ $\frac{y_f}{b_f} = .51$ $\frac{y_f}{b_f} = .72$ $\frac{y_f}{b_f} = .94$

(c) $\Psi = -10^\circ$.

Figure 7.— Continued.

-2

P 0

2

$c_n = 0.24$
c.p. = 108

$c_n = 0$
c.p. = ∞

$c_n = -0.13$
c.p. = -55

$c_n = -0.10$
c.p. = -77

$c_n = 0.09$
c.p. = 187

$\alpha = 6.4°$

-2

P 0

2

$c_n = 1.37$
c.p. = 61

$c_n = 1.12$
c.p. = 61

$c_n = 1.14$
c.p. = 66

$c_n = 0.80$
c.p. = 70

$c_n = 0.97$
c.p. = 65

$\alpha = 12.7°$

○ Upper surface
□ Lower surface

-4

-2

P

0

2

$c_n = 2.28$
c.p. = 55

$c_n = 2.48$
c.p. = 54

$c_n = 2.47$
c.p. = 54

$c_n = 1.99$
c.p. = 57

$c_n = 1.72$
c.p. = 59

$\alpha = 18.9°$

-4

-2

P

0

2

$c_n = 1.97$
c.p. = 51

$c_n = 3.19$
c.p. = 50

$c_n = 3.62$
c.p. = 50

$c_n = 3.27$
c.p. = 51

$c_n = 2.60$
c.p. = 50

0   50   100   0   50   100   0   50   100   0   50   100   0   50   100

Percent flap chord

NACA

$\alpha = 25.1°$

$\frac{y_f}{b_f} = .07$ $\frac{y_f}{b_f} = .29$ $\frac{y_f}{b_f} = .51$ $\frac{y_f}{b_f} = .72$ $\frac{y_f}{b_f} = .94$

(d) $\psi = -20°$.

Figure 7.— Concluded.

Figure 8.— Variation of the normal—force and hinge—moment coefficients across the leading—edge flap span for the 42° sweptback wing. Split flaps deflected; R = 5.12 × 10^6.
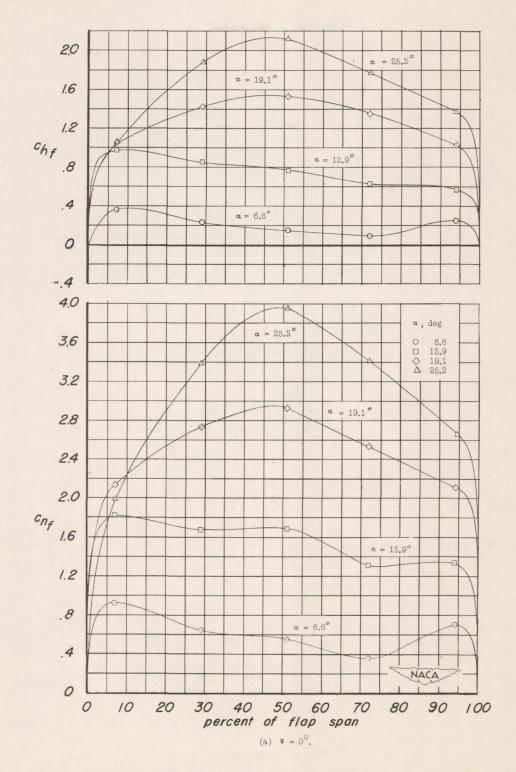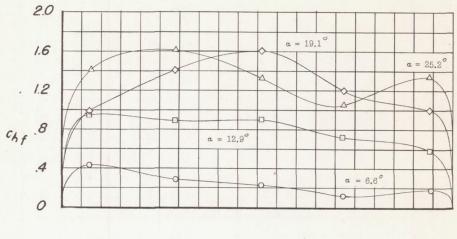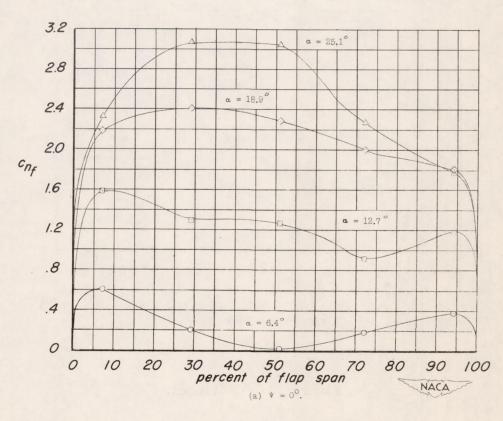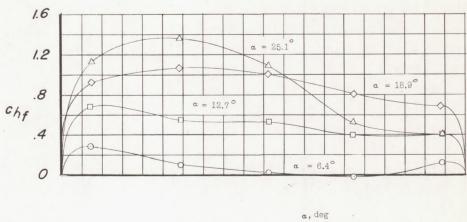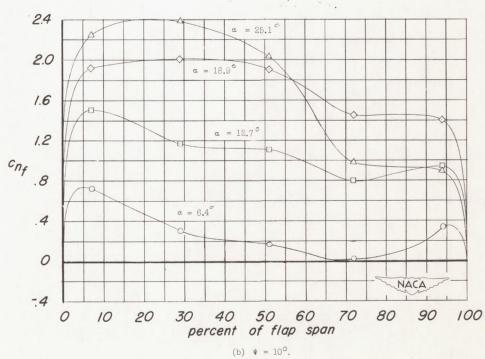
Figure 9.— Variation of the normal—force and hinge—moment coefficients across the leading—edge flap span for the 52° sweptback wing. Split flaps deflected and fences installed; $R = 4.4 \times 10^6$.
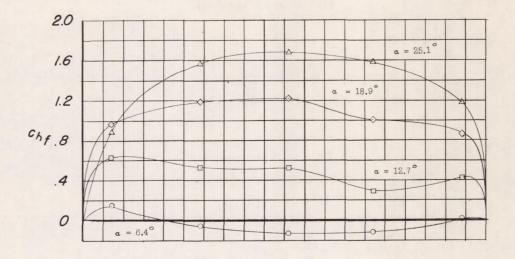
(a) $\Psi = 0°$.

(b) $\Psi = 10°$.

Figure 9.— Continued.

(c) $\Psi = -10°$.

Figure 9.— Continued.

(d) $\Psi = -20°$.
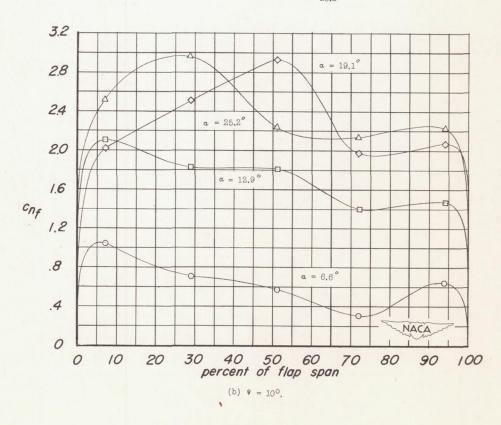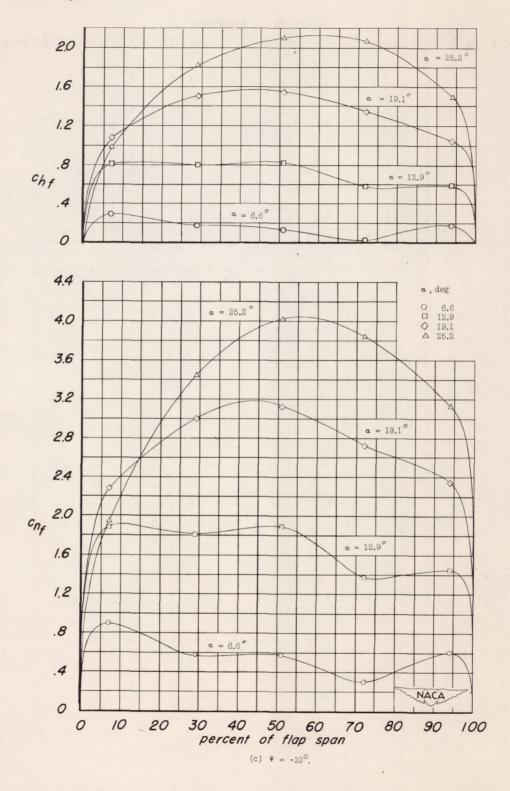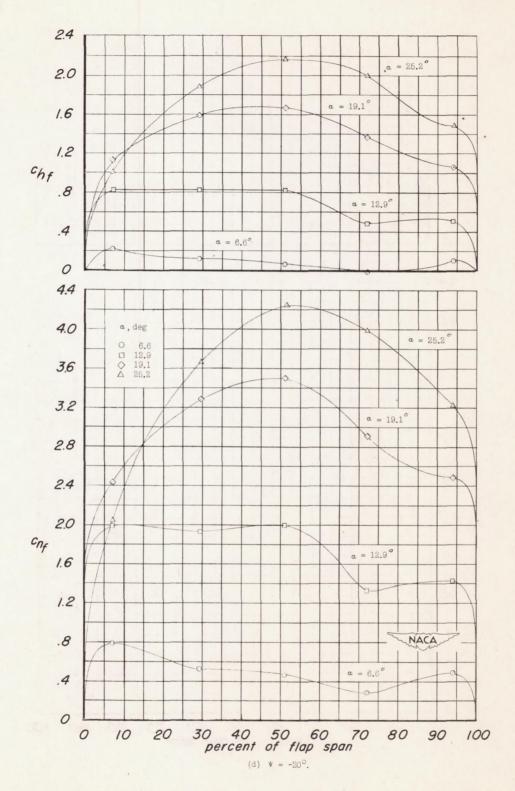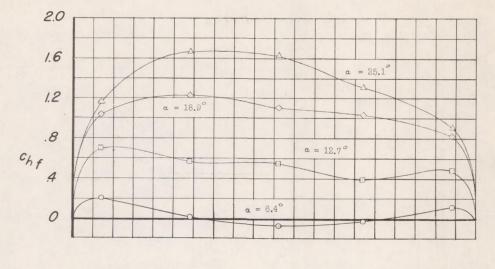
Figure 9.— Concluded.

Figure 10.— Variation of the normal—force and hinge—moment coefficients across the leading—edge flap span for the 52° sweptback wing. Split flaps neutral, fences installed; R = 4.4 × 10⁶.

(b) $\psi = 10°$.

Figure 10.— Continued.

(c) $\psi = -10°$.

Figure 10.— Continued.

(d) $\psi = -20°$.
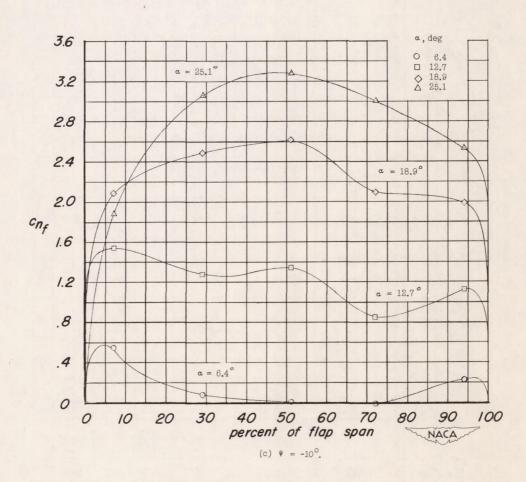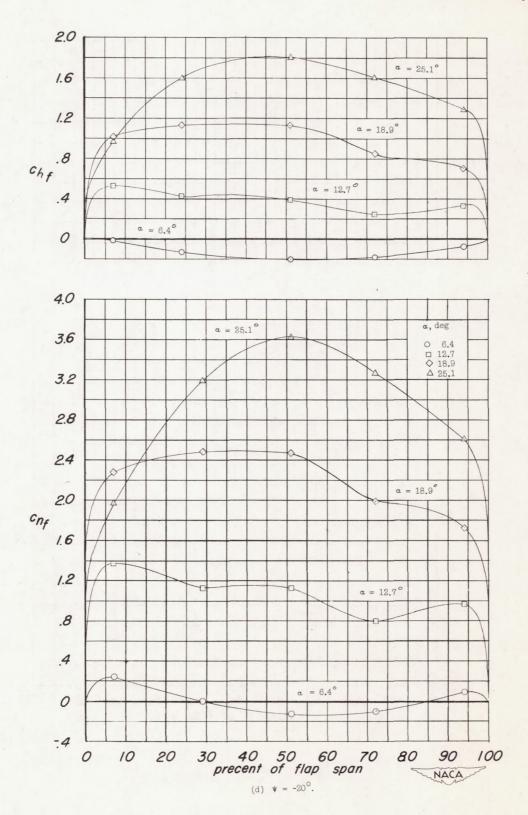
Figure 10.— Concluded.

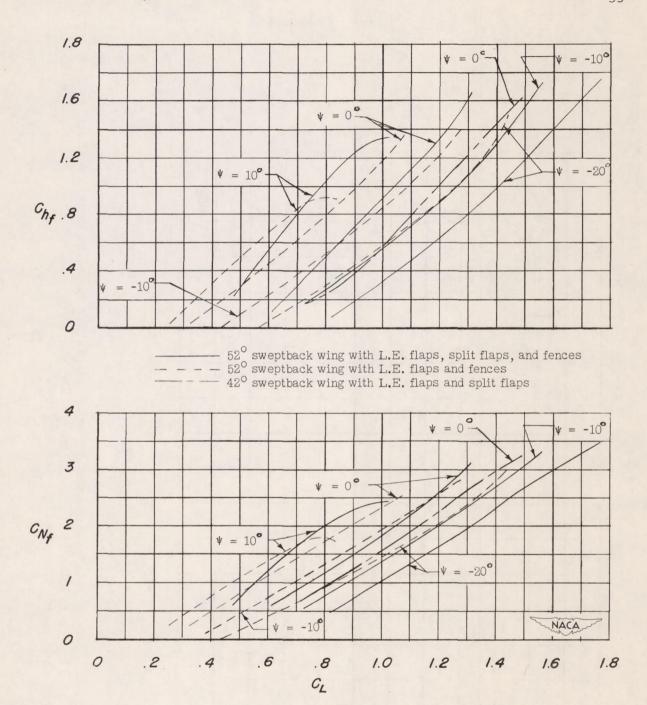Figure 11.— Variation of C_{N_f} and C_{h_f} with C_L for an extended leading-edge flap on wings of 42° and 52° sweepback for various angles of yaw with and without split flaps deflected.
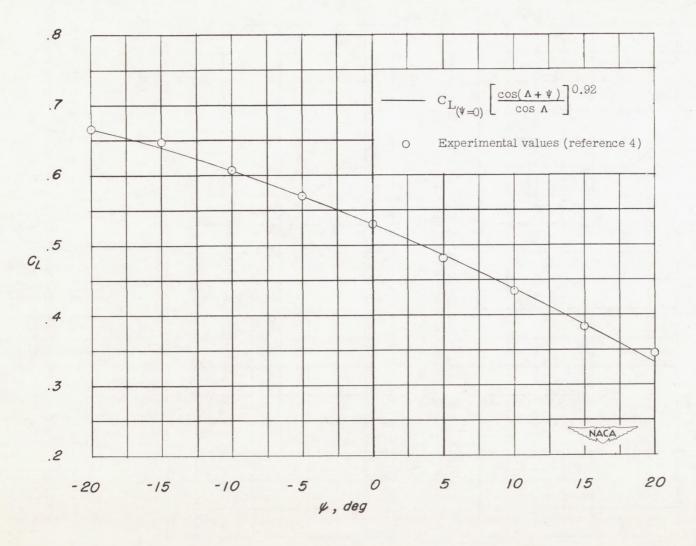
Figure 12.— Comparison of calculated values and experimental values based on pressure distributions for the variation of lift coefficient with angle of yaw for one wing panel of a 45° sweptback wing. (Reference right wing panel.)
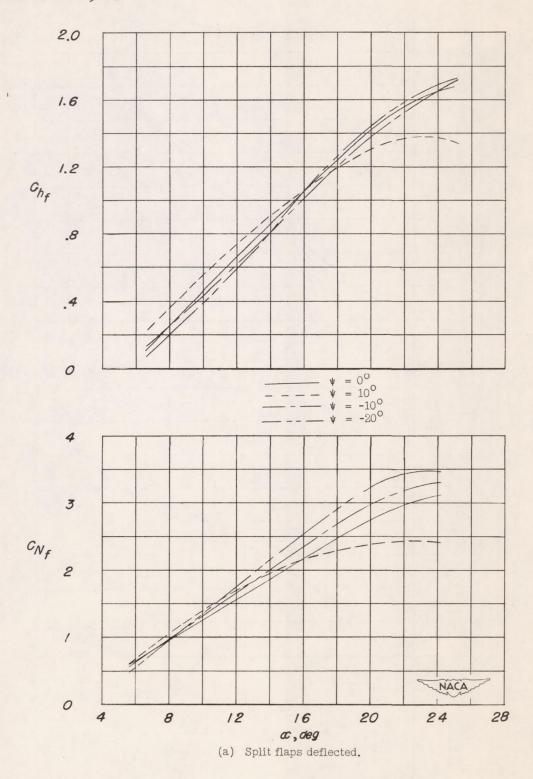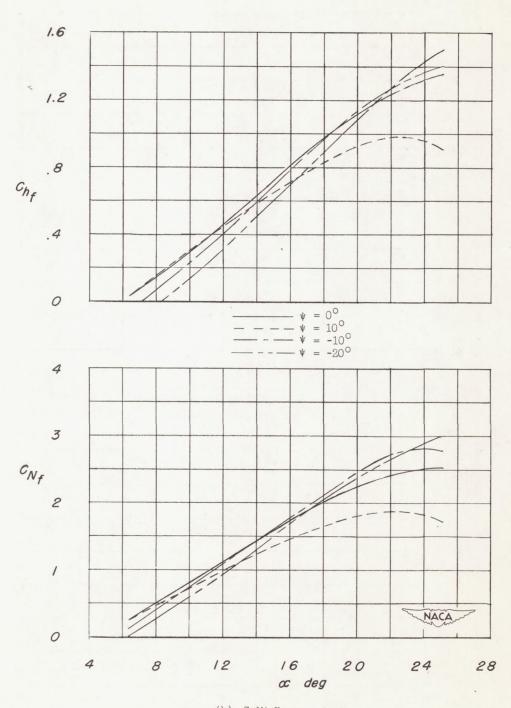
2.0

1.6

1.2

C_{h_f}

.8

.4

0

—————— $\psi = 0°$
– – – – – $\psi = 10°$
–·–·–·– $\psi = -10°$
– – – – $\psi = -20°$

4

3

C_{N_f}

2

1

0

4   8   12   16   20   24   28

α, deg

(a) Split flaps deflected.

Figure 13.— Variation of the total flap normal—force and hinge—moment
coefficients with angle of attack for the 52° sweptback wing and
fences installed; $R = 4.4 \times 10^6$.

1.6

1.2

C_{h_f}

.8

.4

0

—————— $\psi = 0°$
– – – – – $\psi = 10°$
—·—·— $\psi = -10°$
—··—··— $\psi = -20°$

4

3

C_{N_f}

2

1

0

4   8   12   16   20   24   28

α deg

(b) Split flaps neutral.

Figure 13.— Concluded.